DUNITZ, J. D., MAVERICK, E. F. & TRUEBLOOD, K. N. (1988). *Angew. Chem.* **100**, 910–926.
FAGGIANI, R., GILLESPIE, R. J., SAWYER, J. F. & TYRER, J. D. (1980). *Acta Cryst.* B**36**, 1014–1017.
HAMILTON, W. C. (1965). *Acta Cryst.* **18**, 502–510.
HIRSHFELD, F. L. (1976). *Acta Cryst.* A**32**, 239–244.
IBERS, J. A. & HAMILTON, W. C. (1984). *International Tables for X-ray Crystallography*, Vol. IV, pp. 99, 149. Birmingham: Kynoch Press. (Present distributor Kluwer Academic Publishers, Dordrecht.)
JOHNSON, C. K. (1965). *ORTEP*. Report ORNL-3794. Oak Ridge National Laboratory, Tennessee, USA.
JOHNSON, C. K. (1970). *Crystallographic Computing*, edited by F. R. AHMED, pp. 220–226. Copenhagen: Munksgaard.
KIRTLEY, S. W., CHANTON, J. P., LOVE, R. A., TIPTON, D. L., SORRELL, T. N. & BAU, R. (1980). *J. Am. Chem. Soc.* **102**, 3451–3460.
MOTHERWELL, S. (1976). *PLUTO. Program for Plotting Molecular and Crystal Structures*. Univ. of Cambridge, England.
MÜLLER, U., HA-EIERDANZ, M.-L., KRÄUTER, G. & DEHNICKE, K. (1991). *Z. Naturforsch. Teil B*, **46**, 175–182.
NÖTH, H. (1982). *Z. Naturforsch. Teil B*, **37**, 1491–1498.
ROESKY, H. W., DHATHATHREYAN, K. S., NOLTEMEYER, M. & SHELDRICK, G. M. (1985). *Z. Naturforsch. Teil B*, **40**, 240–246.
SCHMIDPETER, A. & WEINGAND, C. (1969). *Angew. Chem.* **81**, 573–574.
SCHOMAKER, V. & TRUEBLOOD, K. N. (1968). *Acta Cryst.* B**24**, 63–76.
SHELDRICK, G. M. (1976). *SHELX*76. *Program for Crystal Structure Determination*. Univ. of Cambridge, England.
SHELDRICK, G. M. (1985). *SHELXS*86. *Program for the Solution of Crystal Structures*. Univ. of Göttingen, Germany.
SPEK, A. L. (1982). *Computational Crystallography*, edited by D. SAYRE, p. 528. Oxford: Clarendon Press.
TRUEBLOOD, K. N. (1978). *Acta Cryst.* A**34**, 950–954.
WILSON, R. D. & BAU, R. (1974). *J. Am. Chem. Soc.* **96**, 7601–7602.

Acta Cryst. (1995). B**51**, 71–76

The *Ab Initio* Crystal-Structure Determination of Perdeuterodimethylacetylene by High-Resolution Neutron Powder Diffraction

BY R. M. IBBERSON

*ISIS Science Division, Rutherford Appleton Laboratory, Chilton, Didcot, Oxon OX*11 0*QX, England*

AND M. PRAGER

Institut für Festköperforschung der KFA Jülich Postfach 1913, *W*5170 *Jülich, Germany*

(*Received* 7 *March* 1994; *accepted* 1 *June* 1994)

Abstract

The low-temperature crystal structure of dimethylacetylene-d_6 (2-butyne-d_6, CD_3—C≡C—CD_3) has been solved *ab initio* from high-resolution neutron powder diffraction data. The structure is monoclinic, space group $C2/m$, with two molecules per unit cell. At 5 K, the cell dimensions are $a = 7.15889$ (4), $b = 6.45529$ (2), $c = 4.07818$ (9) Å and $\beta = 101.0535$ (5)°; $V = 184.97$ Å^3. The powder diffraction pattern for the material exhibits *hkl*-dependent line broadening, apparently as a result of stacking faults intrinsic to the structure. Novel analysis techniques have been used to model line broadening and enable accurate structural parameters to be obtained.

Introduction

Dimethylacetylene (2-butyne, CH_3—C≡C—CH_3) is a simple linear molecule composed of only two different elements. It is, therefore, a model compound for comparing the *ab initio* calculation of methyl-group rotation potentials from structural data with potentials derived from tunnelling and librational transitions [see, for example, work on *p*-xylene (Prager, David & Ibberson, 1991) and toluene (Prager, Monkenbusch, Ibberson, David & Cavagnat, 1993).] For such studies, accurate structural data are a prerequisite. The crystal structure of non-deuterated dimethylacetylene (subsequently referred to as DMA) has been solved using single-crystal X-ray diffraction (Miksic, Segerman & Post, 1959). The proposed structure is tetragonal at low temperature and only the atomic positions for C atoms were determined. On the basis of this structure, using calculated proton positions and reliable pair potentials for pure hydrocarbons (Kitaigorodskii, 1965), a full lattice dynamical calculation was carried out. However, these calculations indicate a completely unstable crystal structure, therefore suggesting incorrect structural parameters for the proton positions and possibly an erroneous

molecular orientation. In order to obtain a reliable base for the calculations, the low-temperature structure has been reinvestigated.

DMA melts at 241 K and thus is a liquid at ambient temperature. Furthermore, specific heat measurements (Yost, Osborne & Garner, 1941) reveal an anomaly at 154 K. Severe technical problems are, therefore, encountered with single crystal techniques. Indeed, the low-temperature structure determination (Miksic *et al.*, 1959) is based on data from only two oscillation photographs, after which the crystal shattered, presumably as a result of the reconstructive nature of the phase transition. Under these circumstances the technique of powder diffraction, particularly at high resolution, offers a useful alternative for detailed structural investigations.

Experimental

A fully deuterated sample, hexadeuterodimethylacetylene or PDMA, was hand-ground at liquid nitrogen temperature under a cold nitrogen gas atmosphere. Approximately 2 cm^3 of the resulting fine powder, contained in a standard 12 mm diameter vanadium sample holder, was loaded into a helium flow 'orange' cryostat. Time-of-flight neutron powder diffraction data were collected on the high-resolution powder diffractometer, HRPD (Ibberson, David & Knight, 1992) at the ISIS pulsed neutron source.* A time-of-flight diffractometer such as HRPD utilizes a polychromatic neutron beam and, therefore, data are recorded by fixed angle detectors. Neutron wavelengths are discriminated by their time of arrival since $t \propto 1/v_n \propto \lambda_n \propto d$, where t is the time of flight, v_n is the neutron velocity, λ_n is the neutron wavelength and d is the d-spacing of a particular Bragg reflection. For the present experiments at backscattering, with $\langle 2\theta \rangle = 168°$, the time-of-flight ranges used were 30–130 and 100–200 ms, corresponding to d-spacing ranges of between approximately 0.6 and 2.6, and 2.0 and 4.0 Å, respectively. Under these experimental settings, the diffraction data have an approximately constant resolution of $\Delta d/d = 8 \times 10^{-4}$.

Diffraction data were recorded at 5 K, in order to minimize the effects of thermal motion, for a period of some 8 h. Data were initially recorded at 170 K in the high-temperature phase prior to slow cooling through the transition point at 154 K, to record a second data set at 120 K in the low-temperature phase. The structural phase transition was clearly observed, but the diffraction data, particularly in the low-temperature phase, showed severe anisotropic line broadening. This *hkl*-dependent broadening is observed in both phases. Subsequent attempts to improve the sample quality by annealing just below T_c proved unsuccessful.

A standard data reduction procedure was followed: the data were normalized to the incident beam monitor profile and corrected for detector efficiency effects using a previously recorded vanadium spectrum.

Structure solution and refinement

Miksic *et al.* (1959) report tetragonal structures for both forms of DMA. In the high-temperature phase at 223 K, the cell dimensions are $a = 5.42$ (2) and $c = 6.89$ (2) Å, whereas the low-temperature form at 138 K exhibits a doubling along the c-axis with cell dimensions of $a = 5.362$ (6) and $c = 13.67$ (3) Å. The molecular volume of DMA in each structure is *ca* 100 $Å^3$. Attempts to index the powder diffraction data in the present study using these cells proved unsuccessful. Accordingly, the first 20 low-order Bragg reflections of the 170 and 120 K data sets were determined by visual inspection, to an accuracy of 0.001 Å, for indexing purposes.

Determination of the unit cells was subsequently carried out using an autoindexing method: *ITO* program (Visser, 1988) on default settings and only the d-spacings of the 20 reflections ($1.5 < d < 3.5$ Å) as input. The results are shown in Table 1. Both solutions gave unique cells with high figures of merit and none of the measured lines remaining unindexed. This ease of lattice parameter determination from first principles is typical of time-of-flight powder diffraction experiments when the highest d-spacing information is available. This is because in time-of-flight measurements the zero-point error is not only small, but becomes progressively less important the larger the d-spacings which have longer times-of-flight, in contrast to the situation in constant wavelength measurements.

The rhombohedral and monoclinic unit cells determined for the respective high- and low-temperature phases are clearly at variance with the previous structural studies. However, there is consistency with respect to the molecular volume. Assuming three molecules per unit cell in the rhombohedral phase and two per unit cell in the monoclinic phase, the molecular volume is calculated at 98.60 and 95.44 $Å^3$, respectively. The possibility for pseudo-orthorhombic and pseudo-tetragonal cells may account for the discrepancies in phase behaviour observed in the present neutron powder diffraction measurements compared with the existing X-ray single-crystal results (Miksic *et al.*, 1959). Unit-cell transformation calculations, permitting an error of up to 1% in the present cell dimensions, yield both

* A list of neutron powder diffraction data has been deposited with the IUCr (Reference: AN0505). Copies may be obtained through The Managing Editor, International Union of Crystallography, 5 Abbey Square, Chester CH1 2HU, England.

Table 1. *Results of the autoindexing for PDMA at* 170 *and* 120 K

T (K)	a (Å)	b (Å)	c (Å)	α (°)	β (°)	γ (°)	Figure of merit	Lattice type
170	6.6778	6.6778	7.6572	90	90	120	103.5	*R*
120	7.0282	6.6580	4.1826	90	99.163	90	51.1	*C*

orthorhombic ($a = 4.08$, $b = 14.12$, $c = 6.45$ Å) and tetragonal ($a = 4.08$, $c = 6.80$ Å) cells.

The high background observed in diffraction data of the rhombohedral phase is most likely a result of diffuse scattering and represents strong evidence of a highly disordered structure. A detailed investigation of this phase and the nature of the phase transition is presently being undertaken. The present work, therefore, concentrates on the low-temperature phase.

The 5 K data were easily indexed assuming a C-centred monoclinic cell, consistent with the 120 K data, suggesting no further phase transitions had occurred below $T_c = 154$ K. Surprisingly, the refined 5 K cell parameter values and measurements taken on cooling the sample revealed that the a lattice parameter increases with decreasing temperature. The systematic absences are consistent with the space groups $C2/m$, $C2$ and Cm. The space group $C2/m$ was chosen for the structure solution following the results of inelastic neutron scattering experiments (Alefeld & Kollmar, 1976). These data indicate all methyl groups to be crystallographically equivalent and thus exclude the possibility of a non-centrosymmetric space group in which two independent molecules are required in order to satisfy molecular volume considerations.

Structure solution

The collapse of three dimensions of diffraction data on to the one dimension of a powder diffraction profile leads to an inevitable peak overlap. The consequent loss of information, particularly at short d-spacings, makes *ab initio* structure solution from powder data inherently difficult. The extraction of reliable structure-factor amplitudes from powder data is, therefore, of crucial importance. Instead of performing a traditional Rietveld profile refinement in which the atomic coordinates, unit-cell and peak-shape parameters are varied, the present method involves the least-squares refinement of unit-cell constants, peak-width parameters and individual peak intensities. This technique was originally pioneered by Pawley (1981) and was carried out using an in-house suite of programs (David, Ibberson & Matthewman, 1992). The method is highly successful in regions of no peak overlap, but the refined intensity values can become highly correlated when substantial overlap occurs. It should be noted that whilst the use of high-resolution powder diffractometers such as HRPD serve to minimize peak overlap, in cases like the present, intrinsic sample-dependent line broadening leads to unavoidable severe overlap. Under these circumstances, the Pawley method will still permit a summed group of Bragg peaks to be well determined, although the individual intensities can have extreme negative and positive values, often larger in magnitude than the overall 'clump' intensity. In the present work, this fundamental weakness of the least-squares method has been overcome using a Bayesian approach formulated by Sivia & David (1994) to extract the structure-factor amplitudes. The Bayesian analysis imposes a positivity constraint to the extraction of structure-factor amplitudes that reduces the effects of correlation. Assuming an arbitrary value of 70% correlation, above which intensity information cannot be reliably extracted, the Bayesian approach permitted the extraction of 413 structure-factor amplitudes, $|F(hkl)|$, compared with 181 from the standard least-squares analysis. Moreover, and of cricial importance for a direct methods solution, the range over which reliable intensity information could be extracted was extended from 0.827 down to 0.633 Å in d-spacing.

A total of 413 reflections were used as input to the direct methods program *MITHRIL* (Gilmore, 1983). The program was run using default parameters. After normalization, 154 of the observed reflections had $|E|$ values >1.0 and were available for the development of phase relationships. A standard direct methods calculation then led to an E-map in which, based on relative peak height, the first four peaks were assigned to atoms. Subsequent peaks showed less than half the height of the fourth peak. The bond lengths and angles between these peaks permitted the assignment of the atoms. It should be noted that for neutrons the scattering factors for carbon and deuterium are essentially equivalent. Attempts at structure solution without recourse to the Bayesian data processing procedure yielded highly ambiguous results.

The structure comprizes one half-molecule per asymmetric unit, consistent with molecular volume calculations and the space group assignment. The atomic coordinates determined in the direct methods calculations were subsequently used as a starting model for the full profile refinement.

Structure refinement

Due to the *hkl*-dependent line broadening in the data, the *SAPS* program (Structure And Peak Shape refinement: David, 1990; David, Ibberson & Matthewman, 1992), a modification of the Rietveld technique was utilized to analyse peak broadening in a model-independent manner.

The mechanism of neutron production and moderation at a spallation source is a complicated process and thus it is not surprising that the pulse shape is of a complex nature. The peak-shape formulation used in the profile refinement models several physical factors, namely pulse shape, moderator physics and instrumental resolution. It may be described as a multiple convolution of several functions that include Lorentzian and Gaussian contributions. Information about size and strain effects within a sample are contained in the convolution of these two functions and, therefore, the peak-shape parameterization is crucial. The most general parameterization of the instrumental peak shape currently used at ISIS is detailed below and reflects the complications of the white beam nature of the neutron radiation

switch (R)	$a_r/[\exp(\lambda/b_r) + \exp(c_r^2/\lambda)]$	(3 parameters)
fast decay (τ_f)	$a_f + b_f\lambda$	(2 parameters)
slow decay (τ_s)	$a_s + b_s\lambda$	(2 parameters)
Gaussian (σ)	$(a_\sigma + b_{\sigma\lambda}^2 + c_{\sigma\lambda}^4)^{1/2}$	(3 parameters)
Lorentzian (Γ)	$(a_\Gamma + b_{\Gamma\lambda} + c_\Gamma\lambda^2)$	(3 parameters).

There is a physical rationale for the peak-shape parameterization. The fast exponential decay and slow exponential decay describe the 'slowing down' of epithermal neutrons and the thermal Maxwellian neutrons, respectively. The switch function R models the change between these two regimes as a function of neutron wavelength. The fast decay, τ_f, is closely linear with wavelength and thus is dominated by the b_f term. The slow decay constant τ_s is essentially independent of wavelength and thus is dominated by the a_s term. The small wavelength-independent Gaussian term is attributable to the finite width of the neutron pulse emerging from *ISIS* ($\sim$0.4 μs), and is normally negligible. The second essentially linear term in λ ($\sigma \approx \lambda$) consists of the geometrical contribution, $\Delta\theta\cot\theta$, from the instrument and the effects of strain in the sample. The third 'quadratic' term in σ may be caused by particle size effects and stacking faults. The wavelength-independent Lorentzian term is negligible. The linear term results from strain in the sample and, to a small extent on HRPD, from instrumental effects. This instrumental contribution arises from the addition of spectra with small differences in geometrical resolution. The Lorentzian contribution that is quadratic in λ results from particle size effects and stacking faults. The convolution of normalized Lorentzian (FWHM = Γ) and Gaussian (second moment = σ^2) functions is called the Voigt function, which may be described in terms of a complex complementary error function (David & Matthewman, 1988).

The resultant instrumental peak shape has a characteristic asymmetry with a steep leading edge. In this study, instead of accounting for the peak width by using a smooth functional variation that is parameterized in time-of-flight as described above, the Gaussian and Lorentzian components of each peak were separately refined. This results in a multi-parameter Rietveld problem. This approach led to a substantial improvement in the profile fitting of the data and has the distinct advantage that no assumptions are made about a particular line-broadening model.

A truncated data set ($50 \le t \le 110$ ms; $0.5 \le d \le 2.2$ Å) was used in the final refinement in order to maintain a manageable number of parameters. This is because the present analysis method involves separate variables to describe the widths of individual peaks which become untenable in regions of high peak density. The refinement included anisotropic displacement parameters for the D atoms and no geometric constraints were required in order to achieve convergence of the least-squares fitting. The results of the profile fitting are illustrated in Figs. 1(*a*) and (*b*) and the final refined structural and profile parameters listed in Table 2. Selected bond

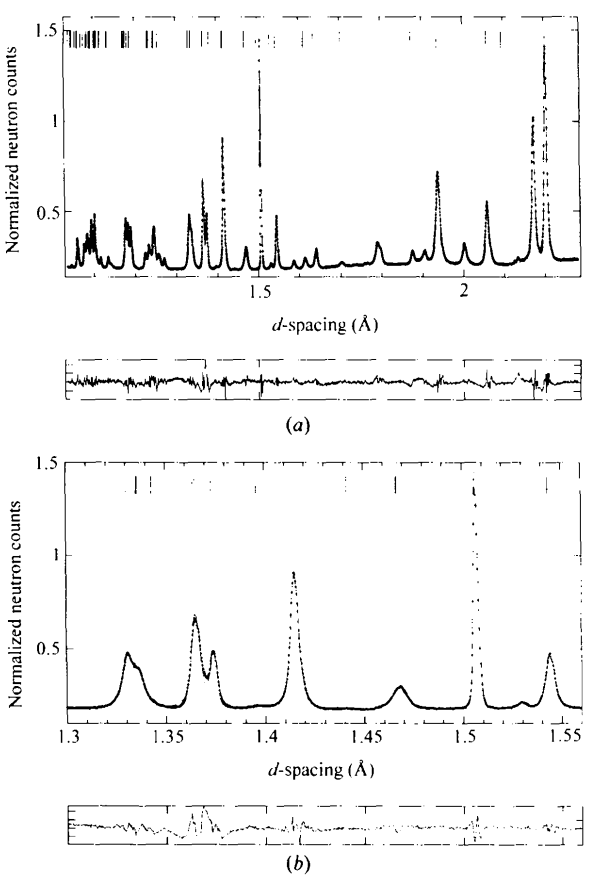

Fig. 1. (*a*) Observed (○), calculated (line) and difference/e.s.d. profiles for PDMA at 5 K. The vertical tick marks represent the calculated peak positions. (*b*). Expanded region of the diffraction profiles highlighting the anisotropic line broadening. The sharp peak at 1.51 Å is the (401) reflection.

Table 2. *Refined structural parameters for PDMA at 5 K*

(*a*) Crystal data and structure refinement

Crystal system	Monoclinic
Space group	*C*2/*m* (No. 12)
a (Å)	7.15889 (4)
b (Å)	6.45529 (2)
c (Å)	4.07818 (9)
β ( )	101.0535 (5)
V (Å^3)	184.97
R_P (%)	2.19
R_{wP} (%)	2.97
R_E (%)	0.82
χ^2 (4778 observations and 66 basic variables)	4.61

(*b*) Atomic coordinates

$$U_{eq} = (1/3)\sum_i \sum_j U_{ij} a_i^* a_j^* \mathbf{a}_i . \mathbf{a}_j .$$

	x	*y*	*z*	U_{eq} (Å^2)*
C(1)	0.0787 (4)	0	0.0839 (6)	0.004 (1)
C(2)	0.2732 (4)	0	0.2810 (10)	0.004 (1)
D(1)	0.2700 (3)	0	0.5475 (10)	0.028 (4)
D(2)	0.3512 (3)	0.1342 (3)	0.2281 (6)	0.024 (2)

(*c*) Anisotropic displacement parameters (Å^2)

	U_{11}	U_{22}	U_{33}	U_{12}	U_{13}	U_{23}
D(1)	0.018 (2)	0.054 (4)	0.011 (2)	0	0.012 (2)	0.000 (1)
D(2)	0.017 (2)	0.018 (2)	0.037 (2)	−0.004 (1)	−0.007 (1)	0.009 (1)

* Values of U_{eq} are quoted for D atoms.

Table 3. *Selected bond lengths* (Å) *and angles* (°)

C(1)—C(1′)	1.201 (4)	C(1)—C(2)	1.468 (4)
C(2)—D(1)	1.091 (6)	C(2)—D(2)	1.075 (3)
C(1′)—C(1)—C(2)	178.5 (3)	C(1)—C(2)—D(1)	110.3 (3)
C(1)—C(2)—D(2)	111.4 (3)		

lengths and angles calculated from the refined atomic coordinates are given in Table 3.

Discussion

The low-temperature crystal structure of the PDMA determined contains only one half-molecule in the asymmetric portion of the unit cell. The full molecular conformation is achieved through an inversion operation, thus all methyl groups are equivalent. This is fully consistent with tunnel splitting of the methyl librational ground state observed by inelastic neutron scattering (Alefeld & Kollmar, 1976). In these experiments, the scattering function relates the elastic incoherent and inelastic structure factors. The respective intensities observed at the momentum transfer given by the instrumental settings exclude the existence of other inequivalent methyl groups.

The bond lengths and angles of the present structure of the low-temperature phase of PDMA are in good agreement with electron diffraction data for DMA (Pauling, Springhall & Palmer, 1939). The accuracy and precision of the structural parameters obtained illustrate well the efficacy and success of the multiparameter profile fitting procedure. The molecule shows a barely significant (5σ) deviation from linearity. The deuterium anisotropic displacement parameters are larger than expected. This probably represents difficulties in modelling structural defects rather than problems with the average structure. The structure is illustrated in Fig. 2(*a*). The molecular axis and one H atom of the methyl group lie in the crystallographic *ac* plane. There is clearly a layering of the molecules within this plane, the precise orientation of the molecules defines the direction along which the structure may shear and provides the key to the origin of the anisotropic line broadening.

Fig. 1(*b*) shows an expanded region of the profile fit. The narrowest peak in the figure, indeed of the whole diffraction profile, is the (401) reflection at a *d*-spacing of 1.51 Å. The anomalously small peak

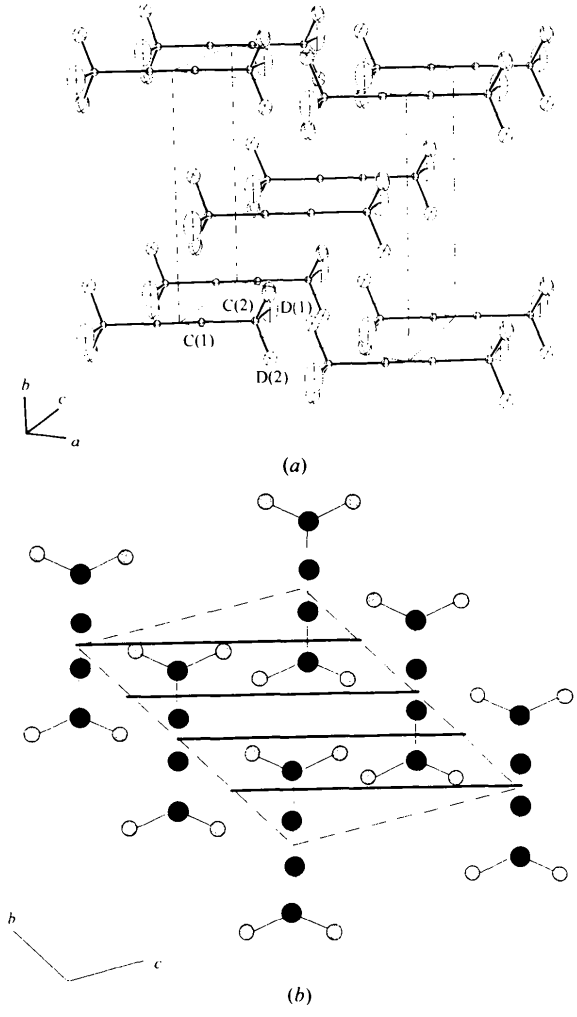

Fig. 2. (*a*) Schematic illustration, drawn using *ORTEP* (Johnson, 1971), of the monoclinic structure of PDMA at 5 K. (*b*) Schematic view of the structure sectioned parallel to the (401) plane. The solid lines represent symmetry-equivalent (401) planes and are seen to be perpendicular to the molecular axis. Dashed lines represent the unit-cell axes.

width is rationalized in terms of the relative insensitivity to the effects of shearing and stacking faults along this plane. Fig. 2(*b*) illustrates the low-temperature structure sectioned parallel to symmetry equivalent (401) planes. It is evident that not only is the (401) plane effectively perpendicular to the molecular axis, it cuts the axis at a near optimum point so as to be relatively insensitive to any along-axis shearing of the structure. Moving away from this plane invokes directions that intersect or are in close proximity to the methyl groups, hence they are likely to be highly disrupted by the suggested stacking fault mechanism and so exhibit line broadening effects.

An initial analysis of the high-temperature rhombohedral phase also shows line-broadening effects and the structural shearing described above may also be invoked to explain the phase transition mechanism. In this model, the highly reconstructive phase transition involves the *a*-axis of the monoclinic phase most likely becoming *c* in the rhombohedral phase.

Preliminary experiments on PDMA were performed at L.L.B., Saclay. One of us (MP) thanks Dr J. Rodriguez for help with this experiment.

References

ALEFELD, B. & KOLLMAR, A. (1976). *Phys. Lett. A*, **57**, 289–290.
DAVID, W. I. F. (1990). *Mater. Res. Soc. Symp. Proc.* **166**, 203–208.
DAVID, W. I. F., IBBERSON, R. M. & MATTHEWMAN, J. C. (1992). Report RAL 92-032. Rutherford Appleton Laboratory.
DAVID, W. I. F. & MATTHEWMAN, J. C. (1988). Report RAL 88-102. Rutherford Appleton Laboratory.
GILMORE, C. J. (1983). *MITHRIL. Computer Program for the Automatic Solution of Crystal Structures from X-ray Data.* Version 1.0. Department of Chemistry, University of Glasgow, Scotland.
IBBERSON, R. M., DAVID, W. I. F. & KNIGHT, K. S. (1992). Report RAL 92-031. Rutherford Appleton Laboratory.
JOHNSON, C. K. (1971). *ORTEP*II. Report ORNL-3794, revised. Oak Ridge National Laboratory, Tennessee, USA.
KITAIGORODSKII, A. I. (1965). *Acta Cryst.* **18**, 585–590.
MIKSIC, M. G., SEGERMAN, E. & POST, B. (1959). *Acta Cryst.* **12**, 390–393.
PAULING, L., SPRINGHALL, H. D. & PALMER, D. H. (1939). *J. Am. Chem. Soc.* **61**, 927–937.
PAWLEY, G. S. (1981). *J. Appl. Cryst.* **14**, 357–361.
PRAGER, M., DAVID, W. I. F. & IBBERSON, R. M. (1991). *J. Chem. Phys.* **90**, 2473–2480.
PRAGER, M., MONKENBUSCH, M., IBBERSON, R. M., DAVID, W. I. F. & CAVAGNAT, D. (1993). *J. Chem. Phys.* **98**, 5653–5661.
SIVIA, D. S. & DAVID, W. I. F. (1994). *Acta Cryst.* A**50**, 703–714.
VISSER, J. W. (1988). *ITO. Autoindexing Program.* Technisch Physische Dienst, PO Box 155, Delft, The Netherlands.
YOST, D. M., OSBORNE, D. W. & GARNER, C. S. (1941). *J. Am. Chem. Soc.* **63**, 3492–3496.

Acta Cryst. (1995). B**51**, 76–80

A New Approach to Structure Resolution by Molecular Dynamics: Variable Force Constants Strategy

BY D. TRANQUI,* J. A. HERMOSO AND M. T. AVERBUCH

Laboratoire de Cristallographie, associé à l'Université Joseph Fourier, CNRS, 25 Avenue des Martyrs, BP 166, 38042 *Grenoble, CEDEX* 09, *France*

AND G. TAMAGNAN, G. LECLERC AND M. CUSSAC

Laboratoire de Chimie Organique, UFR de Pharmacie de Grenoble, Université Joseph Fourier, 5 Avenue de Verdun, BP 138, 38243 *Meylan, CEDEX, France*

(*Received* 22 *March* 1994; *accepted* 14 *July* 1994)

Abstract

Refinement using the 'object-oriented' variation of force constants (VFC) is proven to be an efficient and safe method of refining a molecular structure from a very crude initial model. We illustrate this method by a reinvestigation of the structure of a poorly crystallized compound, *trans*-1,2,3-tris(4-quinolyl)cyclopropane (TQP), which has been recently determined by conventional methods. In the case of TQP, the search model for the VFC method has been obtained by a two-step procedure: (*a*) determination of the most probable conformation of the isolated molecular model by energy-minimization; (*b*) application of the molecular replacement method using the previously computer-designed model as a starting point. The orientation and translation of the molecule were determined, leading to an approximate packing molecular structure. The *R*-factor at

* Author to whom correspondence should be addressed.